IOP Conf. Series: Materials Science and Engineering **428** (2018) 012053 doi:10.1088/1757-899X/428/1/012053

A Novel 2R Parallel Mechanism for Alt-azimuth Pedestal

C C Xu, C Xue and X C Duan*

Key Laboratory of Electronic Equipment Structure Design, Ministry of Education of China, No.2 South Taibai Road Xi'an, China

*E-mail: xchduan@xidian.edu.cn

Abstract. This paper presents a novel 2R parallel mechanism used as alt-azimuth pedestal, i.e. a 2-DOF (degree-of-freedom) pedestal for supporting and rotating equipment about two perpendicular axes. Its active joints are two sliders equipped with servo control on a circular rail. The synchronous and asynchronous motions of the two sliders lead to the azimuth (rotation about the vertical axis) and pitch (rotation about the horizontal axis) of the rotatable platform, respectively. The DOF computation and kinematics are dealt with firstly, and then the dynamic model of the 2R parallel mechanism is established by using the Lagrange equation. Eventually, a numerical simulation of the typical trajectory motion is carried out, and the actuating torque needed in the actuators for the trajectory tracking motion is worked out by employing the derived inverse dynamic equations, which is consistent with the result obtained from commercial software. This study lays a solid base for the further investigation and engineering implementation of the 2R parallel mechanism.

1. Introduction

An alt-azimuth pedestal is an easy-to-realize two-axis pedestal for supporting and rotating equipment such as radar, radio telescope, solar panel about two perpendicular axes[1], i.e., one vertical axis and one horizontal axis. The rotation about the two axes can adjust the azimuth and altitude of the pointing direction respectively. A conventional alt-azimuth pedestal can be described as follows: There are two active perpendicular axes (implemented with two revolute joints) stacked up. Each axis is driven by a servo motor and gear box. It has the advantages of a simple structure and an easy implementation of control modules. However, the joint error accumulation would be very bulky for supporting a heavy rotational platform because of its serial property of the two axes. As an improved structure, another type of alt-azimuth pedestal has a circular rail and several rollers supporting the weight in the azimuth motion[2]. But the serial configuration of the two axes also can increase the power of the azimuth actuator and total weight. It is thus desirable to propose a novel light structure of an alt-azimuth pedestal particularly for the heavy rotational platform.

From the view point of mechanism development, the advantages such as high rigidity, high precision, large load weight ratio, high speed and acceleration of parallel mechanism satisfy the development trend of modern mechanical and electrical equipment with high precision and high speed [3, 4]. Therefore, the parallel mechanism provides a potential solution to the novel light structure of alt-azimuth pedestals. Due to the fact that different degrees of freedom are needed in practical applications, only a few degrees of freedom are needed in some applications, such as 2, 3, 4 or 5 degrees of freedom. Therefore, the lower-mobility parallel mechanism such like the alt-azimuth pedestal has turned to the focus of attention [5]. A planar 2-DOF drive is constructed by introducing a

series of branches and a redundant driver in [6]. Gosselin discussed the application of the 2-DOF parallel robot in the space to a vector which can be used for the tasks of two DOFs [7]. A kind of spherical 2-DOF 5R parallel mechanism, which can be used as the positioning device on the spherical surface, is studied by Zhang and Li et al. [8]. Based on the Lagrange equation, the dynamic model of spherical 5R parallel mechanism is established in [9]. However, according to current publications, there exist no 2R parallel mechanism configuration able to provide the 0-360 (or -180 to 180) degree azimuth motion and ordinary pitch motion for the alt-azimuth pedestal.

This paper presents a novel 2R parallel mechanism used as alt-azimuth pedestal, which two active joints are two sliders with independent servo control on a circular rail. The synchronous and asynchronous motions of the two sliders lead to the azimuth and pitch of the rotatable platform, respectively. The DOF computation, kinematics and dynamics are dealt with firstly; moreover a numerical simulation is also carried out to validate the related results.

2. Structural description

As shown in Figure 1, the 2R parallel mechanism based alt-azimuth pedestal includes a vertical column (8) ,which is connected with ground or an external base; a rotatable platform (7) attached to the column by revolute joints (5) and (9); a horizontal rail (1) with the rack on its inner lateral face; two rods (6) with fixed length, one end of each rod connecting the rotatable platform with a 2-DOF revolute joint(4) and the other end of each rod connecting the sliders (2) with a 3-DOF rotational joint (3). There are prismatic joints between the rail and the sliders. A gear pair attached to the slider engages with the rack and is driven by the servo motor and the reducer.

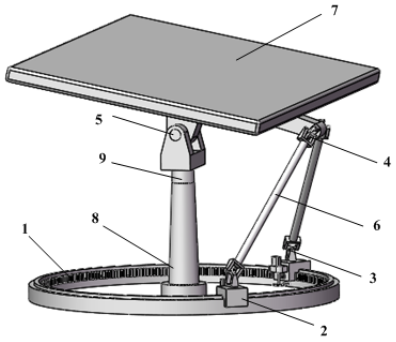

Figure 1. The 2R parallel mechanism based alt-azimuth pedestal.

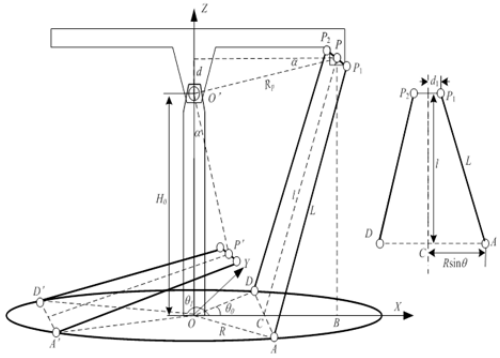

Figure 2. Schematic diagram of the 2R parallel mechanism.

The configuration synthesis of the mechanism is a fundamental process to guarantee the workspace of the rotatable platform. Referring to Figure 2, the directional angles of sliders θ_0 and θ_1 should be determined firstly according to the condition of interference-free when the pitch angle of rotatable platform is 0° and 90°. And then, in order to achieve the pitch angle $\varphi\left(0^\circ \le \varphi \le 90^\circ\right)$ and azimuth angle $\gamma\left(-180^\circ \le \gamma \le 180^\circ\right)$ without interference, the radius of the circular rail R is calculated as follows.

$$R = \frac{H_0\left(R_\mathrm{p}\cos\alpha + d\right)}{d_1\left(\sin\theta_0 - \sin\theta_1\right) - d\cos\theta_1 + R_\mathrm{p}\cos\alpha\cos\theta_0} \tag{1}$$

where, $\alpha = \arcsin\left(dR_\mathrm{p}^{-1}\right)$, d is the height difference of the two revolute joints, d_1 is half of P_1P_2, R_p is the equivalent rotational radius as shown in Figure 2.

The length of the rod L is eventually determined as follows.

$$L = \left[l^2 + \left(R\sin\theta_0 - d_1\right)^2\right]^{1/2} \tag{2}$$

where, $l=\left[(H_0+d)^2+(R_p\cos\alpha-R\cos\theta_0)^2\right]^{1/2}$ is the length of equivalent rod *PC*.

The number of DOF can be calculated according to the modified Kutzbach-Grubler formula [10]

$$M=d(n-g-1)+\sum_{i=1}^{g}f_i+\nu-\zeta=6\times(7-8-1)+14=2 \tag{3}$$

3. Kinematic model

3.1. Inverse orientation solution

The directional angles of sliders *D* and *A* shown in Figure 2 are assumed as θ_1 and θ_2, respectively. It is obviously that the positions of *D* and *A* are symmetric when γ=0°. And at this point, the directional angle of *D*, assumed as $\Delta\theta$, can be obtained as follows by solving the geometrical model.

$$\Delta\theta=\arccos M+\arccos N \tag{4}$$

where, $M=\dfrac{d_1^2+H_0^2+R_p^2+R^2-L^2-2H_0R_p\sin(\varphi-\alpha)}{2R\left[R_p^2\cos^2(\varphi-\alpha)+d_1^2\right]^{1/2}}$, $N=\dfrac{R_p\cos(\varphi-\alpha)}{\left[R_p^2\cos^2(\varphi-\alpha)+d_1^2\right]^{1/2}}$.

Further, the inverse orientation can be derived as follows.

$$\begin{aligned}\theta_1&=\gamma+\Delta\theta\\ \theta_2&=\gamma-\Delta\theta\end{aligned} \tag{5}$$

Figure 3 shows the curves of θ_1 and θ_2 in the case of the pitch angle $\varphi=45^\circ$ and the azimuth angle $0\le\gamma\le45^\circ$. One can observe that the inverse orientation solution is analytical and unique.

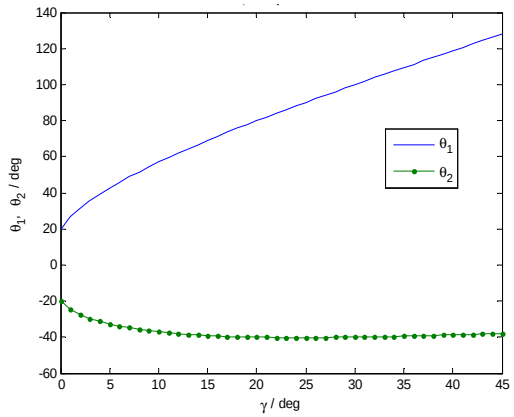

Figure 3. θ_1 and θ_2 vs γ ($\varphi=45^\circ, 0\le\gamma\le45^\circ$).

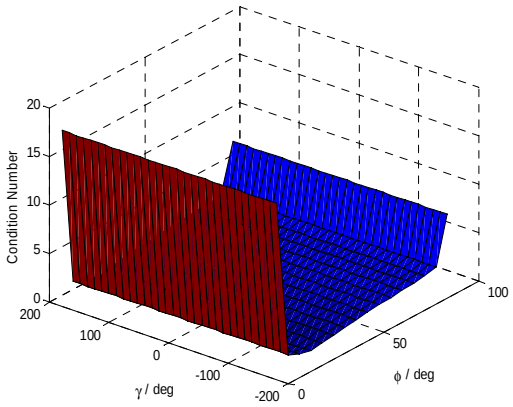

Figure 4. Condition number of the Jacobian matrix.

3.2. Forward orientation solution

Similarly, according to known θ_1 and θ_2, φ and γ can be calculated as follows.

$$\gamma=\frac{\theta_1+\theta_2}{2} \tag{6}$$

$$\varphi=\eta+\alpha-\arccos\lambda \tag{7}$$

where, $\eta=\arccos\dfrac{R\cos\Delta\theta}{\left(R^2\cos^2\Delta\theta+H_0^2\right)^{1/2}}$, $\lambda=\dfrac{d_1^2+H_0^2+R_p^2+R^2-L^2-2d_1R\sin\Delta\theta}{2R_p\left(R^2\cos^2\Delta\theta+H_0^2\right)^{1/2}}$, $\Delta\theta=\dfrac{\theta_1-\theta_2}{2}$.

3.3. Jacobian matrix

The Jacobian matrix of a mechanism is the time-varying mapping coefficient between input and output generalized velocity. The common dexterity index and singularity evaluation function are also derived from the Jacobian matrix. By differentiating Eq. (5) with respect to time, one can obtain

$$\begin{bmatrix} \dot{\theta}_1 \\ \dot{\theta}_2 \end{bmatrix} = [J] \begin{bmatrix} \dot{\varphi} \\ \dot{\gamma} \end{bmatrix} = \begin{bmatrix} \dfrac{\partial \theta}{\partial \varphi} & 1 \\ -\dfrac{\partial \theta}{\partial \varphi} & 1 \end{bmatrix} \begin{bmatrix} \dot{\varphi} \\ \dot{\gamma} \end{bmatrix} \tag{8}$$

Figure 4 shows the condition number in the domain of $-180^\circ \le \gamma \le 180^\circ$ and $0^\circ \le \varphi \le 90^\circ$. One can observe that this 2R parallel mechanism is singularity-free and well conditioned. There is a notable feature that when the pitch angle is fixed, the change of the azimuth angle does not affect its Jacobian matrix condition number, this result agree with our intuition.

4. Dynamic model

The study of mechanism dynamics is to establish the relationship between the driving force and moment of each joint and motion of its output element. Especially, under the condition that the part of the actuator has been given, the force and moment of each driving part and the kinematic pair are solved, which is called dynamic inverse problem [11-13].

4.1. Kinetic energy and potential energy

In order to solve the kinetic energy and potential energy of the mechanism, the mechanism is divided into three parts: the rotational platform, the two rods and the two sliders.

The kinetic energy and potential energy of the rotational platform are

$$K_1 = \frac{1}{2}\left(\boldsymbol{\omega}^T \boldsymbol{I}_s \boldsymbol{\omega}\right),\ P_1 = m_s g z_s \tag{9}$$

where, $\boldsymbol{I}_s$ is the inertia matrix of the coordinate system on the platform with respect to the center of mass, $\boldsymbol{\omega} = \dot{\gamma}\boldsymbol{R}_z(\alpha)\boldsymbol{R}_y(\beta)\vec{x} + \dot{\beta}\boldsymbol{R}_z(\alpha)\vec{y} + \dot{\alpha}\vec{z}$ and m_s are angular velocity and mass of the rotational platform, z_s is the distance from the center of rotational platform to the rail plane.

The kinetic energy and potential energy of the two rods are

$$K_2 = \frac{1}{2}m_l\left(\dot{\boldsymbol{r}}^2_{P_1A} + \dot{\boldsymbol{r}}^2_{P_2D}\right) + \frac{1}{2}J\left(\boldsymbol{\omega}^2{}_{P_1A} + \boldsymbol{\omega}^2{}_{P_2D}\right),\ P_2 = m_l g\left[H_0 - R_p \sin(\varphi - \alpha)\right] \tag{10}$$

where, $\boldsymbol{r}_{P_1A}$ and $\boldsymbol{r}_{P_2D}$ are the position vectors of the rods' centers of gravity, $\boldsymbol{\omega}_{P_1A}$ and $\boldsymbol{\omega}_{P2D}$ are the angular velocity of each rod, m_l is the mass of the rod, $J = \frac{1}{12}m_l L^2$.

The kinetic energy and potential energy of the two sliders are

$$K_3 = \frac{1}{2}m_h\left(\dot{\boldsymbol{r}}^2_A + \dot{\boldsymbol{r}}^2_D\right),\ P_3 = 0 \tag{11}$$

where $\boldsymbol{r}_A$ and $\boldsymbol{r}_D$ are the position vectors of D and A as shown in Figure 2, m_h is the mass of the slider.

4.2. Kinetic equation

The total kinetic energy and potential energy of the system are

$$K = K_1 + K_2 + K_3 = \frac{1}{2}\left(\boldsymbol{\omega}^T \boldsymbol{I}_s \boldsymbol{\omega}\right) + \frac{1}{2}m_l\left(\dot{\boldsymbol{r}}^2_{P_1A} + \dot{\boldsymbol{r}}^2_{P_2D}\right) + \frac{1}{2}J\left(\boldsymbol{\omega}^2{}_{P_1A} + \boldsymbol{\omega}^2{}_{P_2D}\right) + \frac{1}{2}m_h\left(\dot{\boldsymbol{r}}^2_A + \dot{\boldsymbol{r}}^2_D\right) \tag{12}$$

The total potential energy has the following form

$$P = P_1 + P_2 + P_3 = m_s g\left(H_0 + d\cos\varphi\right) + m_l g\left[H_0 - R_p \sin\left(\varphi - \alpha\right)\right] \tag{13}$$

By substituting Eqs. (12) and (13) into Lagrange dynamic equation $\frac{\mathrm{d}}{\mathrm{d}t}\left(\frac{\partial K}{\partial \dot{\theta}_i}\right) - \frac{\partial K}{\partial \theta_i} + \frac{\partial P}{\partial \theta_i} = \tau_i$

A further simplification yields[14]

$$\begin{cases} \tau_1 = \hat{J}_1\ddot{\theta}_1 + \frac{1}{2}\frac{\partial \hat{J}_1}{\partial \theta_1}\dot{\theta}_1^2 + \frac{\partial \hat{J}_1}{\partial \theta_2}\dot{\theta}_1\dot{\theta}_2 + 4\hat{J}_3\ddot{\theta}_2\dot{\theta}_1 + 2\hat{J}_3\dot{\theta}_2^2\ddot{\theta}_1 + \frac{\partial \hat{J}_3}{\partial \theta_1}\dot{\theta}_1^2\dot{\theta}_2^2 + 2\frac{\partial \hat{J}_3}{\partial \theta_2}\dot{\theta}_1\dot{\theta}_2^3 - \frac{1}{2}\frac{\partial \hat{J}_1}{\partial \theta_1}\dot{\theta}_2^2 + \frac{\partial P}{\partial \theta_1} \\ \tau_2 = \hat{J}_2\ddot{\theta}_2 + \frac{1}{2}\frac{\partial \hat{J}_2}{\partial \theta_2}\dot{\theta}_2^2 + \frac{\partial \hat{J}_2}{\partial \theta_1}\dot{\theta}_1\dot{\theta}_2 + 4\hat{J}_3\ddot{\theta}_1\dot{\theta}_2 + 2\hat{J}_3\dot{\theta}_1^2\ddot{\theta}_2 + \frac{\partial \hat{J}_3}{\partial \theta_2}\dot{\theta}_1^2\dot{\theta}_2^2 + 2\frac{\partial \hat{J}_3}{\partial \theta_2}\dot{\theta}_1\dot{\theta}_2^3 - \frac{1}{2}\frac{\partial \hat{J}_2}{\partial \theta_2}\dot{\theta}_1^2 + \frac{\partial P}{\partial \theta_2} \end{cases} \tag{14}$$

Due to space limitation, $\hat{J}_1$, $\hat{J}_2$ and $\hat{J}_3$ in the Eq. (14) are not listed in detail.

5. Numerical simulation

In order to verify the correctness of the dynamic model of the 2R parallel mechanism, the results of the dynamic analysis software and the inverse solution of the dynamic model are compared. The system parameters used in the simulation are shown in the Table 1. The simulation is carried out by using the typical trajectory motion of the rotational platform, which is specified in Eq. (15).

Table 1. The parameters of the 2R parallel mechanism

Symbol	H_0	R_p	R	L	d	d_1	m_s	m_l	m_h	g
Value	5250	3800	4100	5300	1500	3750	70000	8000	1000	9.8
Unit	mm	mm	mm	mm	mm	mm	kg	kg	kg	N/kg

$$\begin{aligned} \dot{\varphi} &= \begin{cases} 5t, 0 \le t < 2 \\ 10, 2 \le t < 8 \end{cases} \\ \dot{\gamma} &= 2t, 0 \le t \le 8 \end{aligned} \tag{15}$$

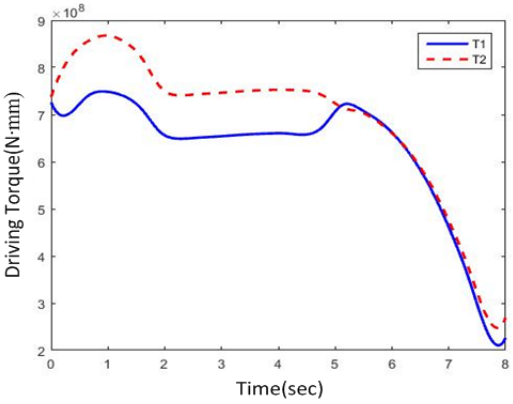

Figure 5. The driving torque of the sliders by calculation.

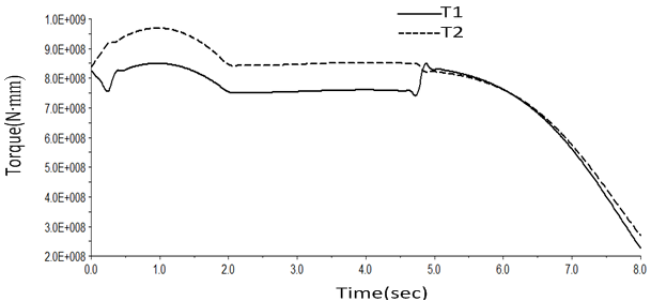

Figure 6. The driving torque of the sliders by simulation.

Figure 5 is the driving torque curves by calculation and Figure 6 is the torque curves by simulation. From the comparison of software simulation and dynamic model calculation, it can be seen the curves basically agrees with each other. The reason for the difference in numerical values arises from the simplification of the kinetic model and the parameter variation such as part mass.

By numerical simulation, the correctness of the dynamic model is verified. In the course of motion

planning, we will be able to carry out simulations of more complicated motion, and consider more reasonable motion planning, so as to minimize the required torque.

6. Conclusions

By introducing a novel 2R parallel mechanism, this paper presents an alt-azimuth pedestal for supporting and rotating a rotational platform about two perpendicular axes. Some meaningful conclusions can be drawn as follows.

(1)The active joints of the 2R parallel mechanism are two sliders with servo control on a circular rail. The synchronous and asynchronous motions of the two sliders lead to the azimuth (Rz) and pitch (Rx) of the rotatable platform, respectively.

(2)The solutions to its inverse and forward orientation problem are both analytical and unique. The 2R parallel mechanism is singularity-free and well-conditioned in its large workspace.

(3)Numerical simulation shows the effectiveness of the dynamic model based on Lagrange equation.

This study lays a solid base for the engineering implementation of the 2R parallel mechanism, which can be extended to other related applications.

Acknowledgments

The authors acknowledge the financial support from the 13th Five-year Plan Advanced Research Project under Grant. 30508040102 and the National Natural Science Foundation of China under Grant. 51679398.

References

[1] Shitov V G 1980 Evalution of the precision in setting a telescope with an alt-azimuth mounting *Measurement Techniques* **23**(1) 16–18
[2] Su D G, Wang Y N and Cui X Q 2004 A configuration for future giant telescope *Acta Astronomica Sinica* **28**(3) 356–366
[3] Huang Z and Kong L F 1997 *Theory and Control of Parallel Robot Mechanism* (Beijing: Machinery Industry Press)
[4] Merlet J P 2006 *Parallel Robots* (Netherlands: Springer)
[5] Huang Z *et al* 2010 Lower-mobility parallel robots: theory and applications *Advances in Mechanical Engineering* **2010**(2) 1652–60
[6] Kock S and Schumacher W 1998 A parallel x-y manipulator with actuation redundancy for high-speed and active stiffness applications *Proc. 1998 IEEE Int. Conf. on Robot and Automation* (Leuven) vol 3 pp 2295–2300
[7] Gosselin C *et al* 1994 Analysis of spherical two degree of freedom parallel manipulators *Proc. of the 23rd Biennial Mechanisms Conf.* (Minneapolis) pp 255–262
[8] Zhang L J, Li Y Q and Huang Z 2006 On the kinematics analysis of a 2-degree-of-freedom spherical 5r parallel manipulator *China Mechanical Engineering* **17**(4) 343–346
[9] Bozorgi E R J *et al* 2014 Design, development, dynamic analysis and control of a 2-degree-of-freedom spherical parallel mechanism *2nd RSI/ISM Int. Conf. on Robotics and Mechanics* (New York) pp 445-450
[10] Yang Y Z, Cheng B and Duan X C 2016 Modeling and analysis of two-degrees-of-freedom spherical parallel manipulator *World Sci-Tech R and D* **5** 1054–59
[11] Craig J J 2004 *Introduction to robotics: mechanics and control* (Upper Saddle River: Prentice Hall)
[12] Liu S Z *et al* 2014 Kinematics and dynamics analysis of a three degree-of-freedom parallel manipulator *Journal of Central South University* **21**(7) 2660–66
[13] Zhang D 2010 Parallel Robotic Machine Tools (The United States: Springer)
[14] Liu S Z *et al* 2009 Kinematic and dynamic analysis of a three-degree-of-freedom parallel manipulator *Journal of Mechanical Engineering* **45**(8) 11–17